Bone 120 (2019) 495–503

Contents lists available at ScienceDirect

Bone

journal homepage: www.elsevier.com/locate/bone

Full Length Article

Sclerosing bone dysplasias with hallmarks of dysosteosclerosis in four patients carrying mutations in *SLC29A3* and *TCIRG1*

Antonia Howaldt[a], Sheela Nampoothiri[b], Lisa-Marie Quell[a], Ayse Ozden[c], Björn Fischer-Zirnsak[a], Corinne Collet[d], Marie-Christine de Vernejoul[e,f,g], Hakan Doneray[c], Hülya Kayserili[h], Uwe Kornak[a,i,j,*]

[a] *Institut für Medizinische Genetik und Humangenetik, Charité – Universitätsmedizin Berlin, corporate member of Freie Universität Berlin, Humboldt-Universität zu Berlin, and Berlin Institute of Health, Berlin, Germany*
[b] *Amrita Institute of Medical Sciences & Research Centre, Cochin, India*
[c] *Ataturk University Faculty of Medicine, Erzurum, Turkey*
[d] *Service de Biochimie et Biologie Moléculaire, CHU Paris-GH St-Louis Lariboisière F. Widal - Hôpital Lariboisière, Paris, France*
[e] *INSERM U1132 BIOSCAR, Hôpital Lariboisière, 75010 Paris, France*
[f] *University Paris Diderot, Sorbonne Paris Cité, Paris, France*
[g] *Service de Rhumatologie, GH Saint-Louis Lariboisière Fernand Widal, Paris, France*
[h] *Medical Genetics Department, Koç University School of Medicine (KUSOM), Istanbul, Turkey*
[i] *Max Planck Institute for Molecular Genetics, Berlin, Germany*
[j] *Berlin-Brandenburg Center for Regenerative Therapies, Charité – Universitätsmedizin Berlin, Freie Universität Berlin, Humboldt-Universität zu Berlin, and Berlin Institute of Health, Berlin, Germany*

ARTICLE INFO

Keywords:
TCIRG1
SLC29A3
Autosomal recessive osteopetrosis
Dysosteosclerosis
Platyspondyly
Next generation sequencing

ABSTRACT

The osteopetroses and related sclerosing bone dysplasias can have a broad range of manifestations. Especially in the milder forms, sandwich vertebrae are an easily recognizable and reliable radiological hallmark. We report on four patients from three families presenting with sandwich vertebrae and platyspondyly. The long bone phenotypes were discordant with one patient showing modeling defects and patchy osteosclerosis, while the second displayed only metaphyseal sclerotic bands, and the third and fourth had extreme metaphyseal flaring with uniform osteosclerosis. Two of the four patients had experienced pathological fractures, two had developmental delay, but none showed cranial nerve damage, hepatosplenomegaly, or bone marrow failure. According to these clinical features the diagnoses ranged between intermediate autosomal recessive osteopetrosis and dysosteosclerosis. After exclusion of mutations in *CLCN7* we performed gene panel and exome sequencing. Two novel mutations in *SLC29A3* were found in the first two patients. In the third family a *TCIRG1* C-terminal frameshift mutation in combination with a mutation at position +4 in intron 2 were detected. Our study adds two cases to the small group of individuals with *SLC29A3* mutations diagnosed with dysosteosclerosis, and expands the phenotypic variability. The finding that intermediate autosomal recessive osteopetrosis due to *TCIRG1* splice site mutations can also present with platyspondyly further increases the molecular heterogeneity of dysosteosclerosis-like sclerosing bone dysplasias.

1. Introduction

Sclerosing bone dysplasias can have a broad range of manifestations with autosomal recessive infantile malignant osteopetrosis at the one end and barely detectable bone mass alterations and/or absence of clinical signs in mild autosomal dominant osteopetrosis or osteomesopyknosis at the other end of the spectrum [12,24,30]. The underlying disease mechanism can be either increased activity of osteoblasts or decreased function of osteoclasts. The former case applies to the disease category hyperostosis with the craniotubular dysplasias as prominent examples, and the latter mechanism is at work in the case of the osteopetroses and related conditions like dysosteosclerosis

Abbreviations: ARO, autosomal recessive osteopetrosis; DOS, dysosteosclerosis; OP, osteopetrosis; TCIRG1, T-cell immune regulator 1; SLC29A3, solute carrier family 29 member 3; WES, whole exome sequencing

* Corresponding author at: Institute of Medical Genetics and Human Genetics, Charité-Universitaetsmedizin Berlin, Augustenburger Platz 1, 13353 Berlin, Germany.
E-mail address: uwe.kornak@charite.de (U. Kornak).

https://doi.org/10.1016/j.bone.2018.12.002
Received 24 September 2018; Received in revised form 1 December 2018; Accepted 6 December 2018
Available online 08 December 2018
8756-3282/ © 2018 Elsevier Inc. All rights reserved.

[4,20]. An important indicator of impaired osteoclast function is sclerosis of the vertebral endplates due to non-resorbed mineralized cartilage leading to the radiological appearance of sandwich vertebrae.

Autosomal recessive osteopetrosis (ARO, OMIM #259700) is in the majority of cases caused by mutations in the T-cell immune regulator 1 (*TCIRG1*) gene and mostly has a lethal course if not timely treated by stem cell transplantation [33]. Due to the absence of a bone marrow cavity in ARO sandwich vertebrae are better seen in intermediate autosomal recessive osteopetrosis or autosomal dominant osteopetrosis type 2 (ADO2, OMIM #166600) that are mainly caused by biallelic or heterozygous mutations in *CLCN7*, respectively [3,5,7]. In rare cases, however, a similar phenotype can also be secondary to intronic mutations in *TCIRG1* [28,37].

Dysosteosclerosis (DOS, OMIM #244300), first described by Spranger et al., is also characterized by sandwich vertebrae and overlaps with intermediate ARO and ADO2 [34]. Additional features include platyspondyly, metaphyseal osteosclerosis and widening, sometimes reminiscent of Pyle's disease, short stature, pathological fractures, cranial nerve damage, hypodontia and impaired tooth calcification, and macular skin changes [4]. In two patients with this diagnosis biallelic mutations in *SLC29A3* were identified, encoding for the equilibrative nucleoside transporter 3 (ENT3), which transports nucleosides and free purine and pyrimidine bases across the lysosomal and mitochondrial membranes [15]. Mutations in *SLC29A3* are more often associated with histiocytosis-lymphadenopathy plus syndrome (OMIM #602782). Major features of this complex disease (generalized inflammation, histiocytic plaques, hepatosplenomegaly, lymphadenopathy) can be attributed to impaired macrophage function and increased proliferation [15]. In contrast, when monocytes from DOS patients were differentiated *in vitro* reduced osteoclast numbers were observed [4,36]. It is still debated whether dysosteosclerosis is an own disease entity or whether the osteosclerotic phenotype associated with *SLC29A3* mutations is just a special manifestation within the histiocytosis-lymphadenopathy disease spectrum. Moreover, in one patient diagnosed with DOS a homozygous intronic mutation in *TNFRSF11A* encoding RANK was identified, which increases the genetic heterogeneity of this phenotype [13]. We describe four patients from three families with sandwich vertebrae, variable platyspondyly, and metaphyseal flaring and sclerosis. We show the similarities between intermediate ARO caused by intronic *TCIRG1* mutations and DOS caused by *SLC29A3* mutations, compare these findings to the literature, and discuss the heterogeneity of dysosteosclerosis its role as a separate disease entity.

2. Material and methods

2.1. Next generation sequencing

Before next generation sequencing was initiated, mutations in *CLCN7* were excluded using Sanger sequencing. For Patients 1 and 2, a custom bone mass panel containing 70 genes known or suggested to cause alterations in bone mineral density was employed [27]. The enrichment of the coding regions of these genes was performed using SureSelect XT target enrichment system from Agilent or NEB-Next DNA Library Prep Master Mix Set from Illumina. Samples were run on an Illumina HiSeq1500 sequencer. On average 92–99% of the target region were covered by at least 20 reads. The resulting reads were mapped to the reference genome (hg19) with Burrows-Wheeler Aligner (BWA). PCR duplicates were removed using Picard and GATK [25] was used to perform realignment around indels and base score recalibrations. Variants were detected by Gene-Talk platform [16,35]. Variant analysis was restricted to all genes known at the time of analysis to cause high bone mass disorder. The pathogenic potential of individual candidate variants was evaluated by MutationTaster [31].

For Patients 3 and 4, libraries for whole exome sequencing (WES) were prepared using NEBNext DNA Library Prep Master Mix Set for Illumina (New England Biolabs). Enrichment of the target regions was done using the SureSelect Human Exome Kit V4 (Agilent Technologies) and run on a HiSeq 1500 Sequencer (Illumina). The average sequencing depth was above 40× and more than 90% of the exome target region was covered by more than 10 reads. Variants were detected with GATK toolkit version 2.6 and the exome genotyping accuracy was estimated to be above 0.9999 based on the variant calls. Variants were detected with SAMtools, annotated with ANNOVAR and finally analysed using the Gene-Talk platform [16]. The pathogenic potential of individual candidate variants was evaluated by MutationTaster [31].

2.2. Sanger sequencing

All 25 exons of the gene *CLCN7* were sequenced by the Sanger method as described before [19]. To validate the variants acquired by bioinformatic filtering of the gene-panel or WES sequencing data, the respective exons and exon–intron boundaries of *SLC29A3* (NM_001174098) and *TCIRG1* (NM_006019) were amplified using oligonucleotide primers (sequences available upon request) and sequenced on an ABI3730xl DNA Analyzer (Applied Biosystems). In this way, the gene regions of the mutations and adjacent regions were depicted and mutations verified, both in the index and family members whenever respective DNA was available.

3. Results

3.1. Clinical presentation of four individuals with sclerosing bone phenotypes

Four patients from three different families presented with osteosclerosis and long bone modeling defects suggesting the diagnosis intermediate autosomal recessive osteopetrosis or dysosteosclerosis (Table 1).

Patients 1 and 2 were of Turkish origin. Patient 1 was a 22-year-old female and the third child born to first-degree cousins. She had two healthy sisters and was the only one affected in the family. Patient 2 was a 11-year-old girl born to first-degree cousins. Her two elder sisters and parents had no phenotype suggestive for osteopetrosis. Patient 3 and 4 were siblings of Indian origin born to non-consanguineous parents. Patient 3 was a 15-year-old boy and his clinically affected 10-year-old sister is referred to as Patient 4. A brother and the parents had an unremarkable phenotype. Patient 1 had short stature (147 cm) and her arm span of 158 cm indicated truncal shortness. However, also the father (160 cm) and one healthy sibling (149 cm) were below the 3rd centile. Patient 2 was at the 3rd centile for height since early childhood. Patient 3 and 4 had clear short stature below the 3rd centile.

A mild global developmental delay and gross motor delay was described for Patients 2 and 3 and failure to thrive was noted in Patients 3 and 4. Skin signs like hypertrichosis or hyperpigmentation as well as macrocephaly, hydrocephaly, or optic nerve compression were absent in all patients. Neither observed were anemia, pancytopenia, hepatosplenomegaly, and recurrent infections.

3.2. Radiological phenotype

Since the radiological phenotype of the siblings Patient 3 and 4 is nearly identical only data for Patient 3 is shown while the existing X-rays for Patient 4 can be found in Supplementary Fig. 1. All four patients had similarly pronounced sandwich vertebrae (Fig. 1). However, platyspondyly was most pronounced in Patient 1 (Fig. 1A) and significantly weaker in Patients 2 to 4 (Fig. 1C, E). Moreover, only Patient

Table 1
Clinical presentation of four individuals with intermediate osteopetrosis and platyspondyly.

	Pt 1	Pt 2	Pt 3	Pt 4	Campeau et al.	Whyte et al.
Gender	Female	Female	Male	Female	Female	Female
Age today	22 y	11 y and 2 months	10 y	5 y	n.d.	10 y
Ethnicity	Turkish	Turkish	Indian	Indian	n.d.	Turkish
Consanguinity	Yes	Yes	No	No	Yes	No
Affected siblings	No	No	Yes	Yes	n.d.	No
Gene	**SLC29A3**		**TCIRG1**			**SLC29A3**
Mutation(s)	c.302_303insCTACTTTGAGAGCTACCT (p.Asn101delins)	c.1172C > A (p.Pro391His)	c.117 + 4A > C (paternal) c.2380_2381delCT (p.Ala796fs*34) (maternal)		(c.1346C > G) p.Thr449Arg	c.607T > C (p.Ser203Pro) c.1157G > A (p.Arg386Gln)
Zygosity	Homozygous	Homozygous	Compound heterozygous		Homozygous	Compound heterozygous
Clinical manifestations (HPO terms)						
Sandwich appearance of vertebral bodies (HP:0004618)	Yes	Yes	Yes	Yes	Yes	Yes
Flattened vertebrae (HP:0000926)	Yes	Yes	Yes	Yes	Yes	Yes
Erlenmeyer flask deformity of the femurs (HP:0004975)	No	No	Yes	Yes	Yes	Yes
Coxa vara (HP:0002812)	Yes	Yes	Yes	Yes	Yes	Yes
Fractures of the long bones (HP:0003084)	Yes (7 fractures femora)	No	No	Yes (clavicle)	Yes	Yes
Dense metaphyseal bands (HP:0100959)	Yes	Yes	Yes	Yes	Yes	Yes
Short stature (HP:0004322)	< 3rd centile	3rd centile (borderline)	< 3rd centile	< 3rd centile	Yes	Yes
Thickened ribs (HP:0000900)	Yes	Yes	Yes	Yes	Yes	Yes
Osteosclerosis of the calvaria and base of the skull (HP:0005746)	Yes	Yes	Yes	Yes	Yes	Yes
Frontal bossing (HP: HP:0002007)	No	No	Yes	No	No	Yes
Prominent supraorbital ridges (HP:0000336)	Mild	Yes	No	No	n.d.	Yes
Narrow face (HP:0000275)	No	Yes	Yes	No	n.d.	Yes
Optic nerve compression (HP:0007807)	No	No	No	No	No	No
Failure to thrive (HP:0001508)	No	No	Yes	Yes	No	No
Motor delay (HP:0001270)	No	Yes	Yes	No	No	No
Mild global developmental delay (HP:0011342)	No	Yes	Yes	n.d.	No	No
Anemia (HP:0001903)	Yes (intermittent)	No	No	No	No	No
Hepatosplenomegaly (HP:0001433)	No	No	No	No	n.d.	n.d.
Abnormality of the teeth (HP:0000164)	Yes (poorly calcified)	Yes	No	No	No	Yes
Hyperpigmentation of the skin (HP:0000953)	No	No	No	No	No	Yes
Recurrent infections (HP:0002719)	No	No	No	No	Yes	Yes

n.d. = not determined.

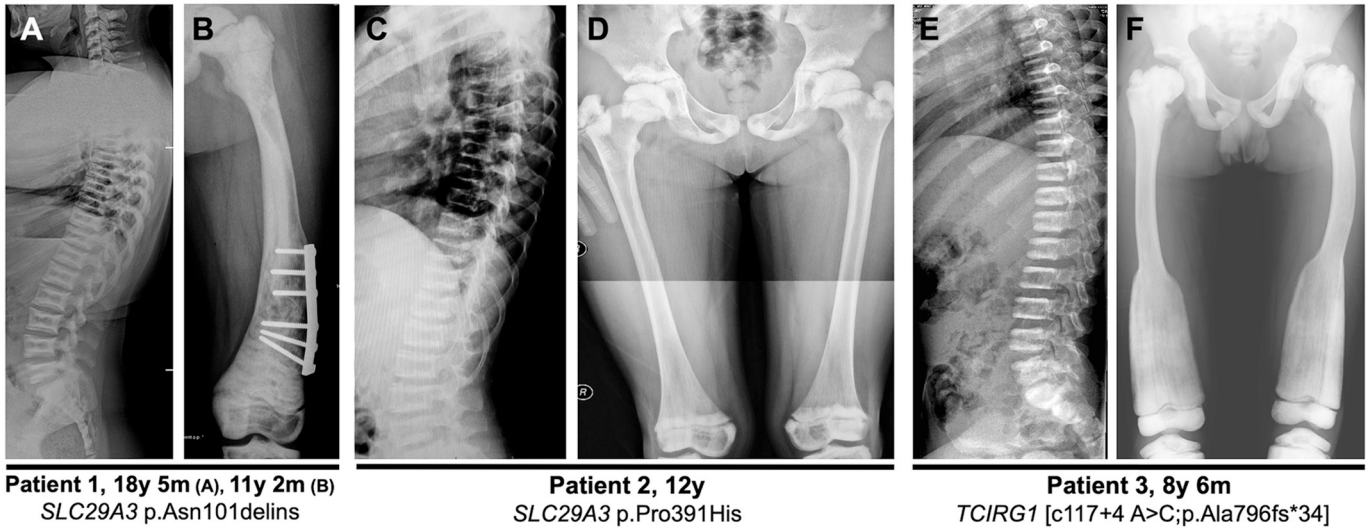

Fig. 1. Radiographs of spine and lower extremities. Patient 1 (A, B) presents with diffuse osteosclerosis, reduced translucency in the long bones and pathologic fractures (osteosynthesis material present). The shape of the femur is altered, it appears to be shortened and broadened. The vertebral endplates are dense and the vertebrae flattened. Patient 2 (C, D) reveals sclerosis of the proximal femur, the pelvis and vertebrae, which are mildly flattened. Patient 3 (E, F) presents with bilateral sclerosis of long bones in lower limbs, a modeling defect, Erlenmeyer flask shaped deformity of the tibia, metaphyseal flaring of tibia and femur, and flattened sandwich vertebrae.

1 showed an irregular concave vertebral shape and a bone-within-bone appearance. Thickened ribs were present in all four patients (Fig. 1A, C, E).

Sclerosis of the long bones was strikingly discordant among the four patients. Patient 1 showed patchy metaphyseal osteosclerosis of the femur, humerus, radius, and ulna (Figs. 1B, 2A). The phalanges showed doubled osteosclerotic bands that resulted in a bone-within-bone appearance (Fig. 2B). In Patient 2 narrow sclerotic bands below the growth plate of the proximal and distal femur and the proximal humerus were evident (Figs. 1D, 2C). The phalanges appeared opaque with only very faint metaphyseal sclerotic bands (Fig. 2D). Patients 3 and 4 presented with a rather uniform osteosclerosis of the femora, tibiae and fibulae (Fig. 1F), and prominent sclerotic bands in the metaphyses of metacarpals and phalanges (Fig. 2F). All patients displayed coxa vara (Fig. 1B, D, F). Fractures were reported in Patients 1 and 4. In Patient 1 the supracondylar region of the right femur was fractured at the age of two years. In the following she had in total seven fractures of both femurs, which were surgically treated three times, at the age of

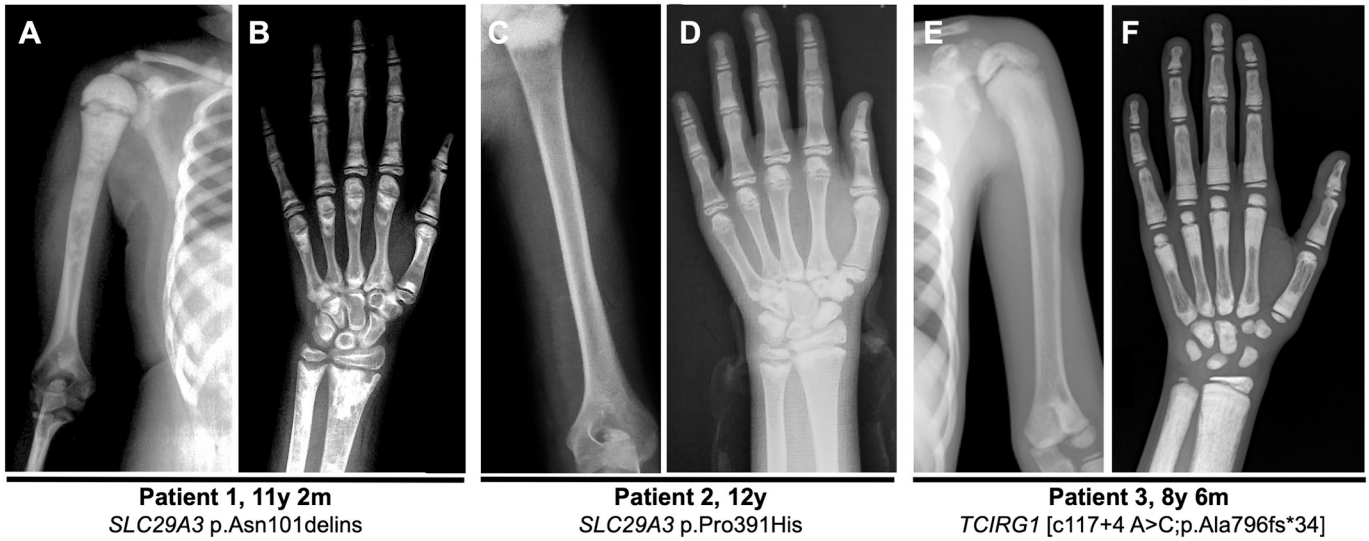

Fig. 2. Upper limb radiographs of Patient 1, 2 and 3. (A) Patient 1 presents with sclerotic foci of the humerus in the proximal two thirds and increased corticalis in the distal third of the humerus. The humerus appears slightly broadened and shortened. (B) Radii and ulnae reveal distinct osteosclerosis and a cloudy appearance. Osteosclerotic bands are predominantly present at the growth plates (C) Patient 2 presents with cortical thickening of the humeri and (D) diffuse sclerosis of the digiti, predominantly visible at methaphyseal regions. (E) In Patient 3, the proximal humerus reveals sclerosis and an abnormal curvature. (F) Strong sclerotic bands are present at distal radius and ulna, at the distal end of the metacarpals and the proximal ends of the phalanges.

eight, 12 and 13 years, respectively, with open reduction and internal fixation with plates and screws (Fig. 1B). Patient 4 experienced a fracture of the clavicle at the age of two years.

Long bone modeling defects were most prominent in Patients 3 and 4, who showed extreme metaphyseal flaring leading to Erlenmeyer shaped femora and broadening of the metaphyses of the upper limb bones and abnormal curvature of the humerus (Fig. 1F; Fig. 2E). In Patient 1 femoral shape appeared also altered with overall shortening and broadening in the presence of fractures which complicate the evaluation (Fig. 1B). A mild broadening and shortening was also evident in the humerus in absence of fractures (Fig. 2A). In Patient 2 no modeling defects were visible (Figs. 1D; 2C, D).

Sclerosis of the skull base was noted in all patients (Fig. 3A–E) (Supp. Fig. 1). Calvarial thickening was evident in Patients 2–4. Prominent supraorbital ridges and a narrow face were present in Patient 2 and 3; abnormalities of the teeth (not further specified) were only observed in Patient 2 (Table 1).

In the light of these clinical and radiological findings we speculated that Patient 2 might have autosomal dominant osteopetrosis type 2, whereas for the other patients the diagnoses intermediate autosomal recessive osteopetrosis or dysosteosclerosis seemed more likely.

3.3. Mutation analysis

After exclusion of mutations in *CLCN7* as the most likely candidate gene for intermediate and autosomal dominant osteopetrosis, gene panel or whole exome sequencing (WES) were carried out, respectively.

In Patient 1 the homozygous mutation *SLC29A3* c.302_303insCTA CTTTGAGAGCTACCT (p.Asn101delinsAsnTyrPheGluSerTyrLeu) was revealed by gene panel sequencing of the most common genes associated with pathological bone mass changes and confirmed by Sanger sequencing (Fig. 4A) [27]. The parents both carried the variant in a heterozygous state. One of the index' phenotypically unaffected sisters was a heterozygous carrier. Gene panel sequencing also detected the homozygous mutation *SLC29A3* c.1172C > A (p.Pro391His) in exon 6 in Patient 2 (Fig. 4B). No segregation analysis was possible due to absence of DNA samples from further family members. Both *SLC29A3* mutations have not been described before in literature. The insertion found in Patient 1 was neither annotated in ExAC nor in the 1000 Genomes project and ranked disease causing by MutationTaster. The missense mutation in Patient 2 was ranked disease-causing by MutationTaster, PolyPhen, and SIFT. The mutation occurred twice in ExAC in a heterozygous state and has not been detected in the 1000 Genome Project. In the ENT3/SLC29A3 topology model (Fig. 4C) the two mutations lie in the loop between transmembrane helices 1 and 2 and in transmembrane helix 9, respectively. A protein alignment shows complete evolutionary conservation of p.Pro391 (Fig. 4D).

In WES data of Patient 3, the compound heterozygous mutations *TCIRG1* c.117 + 4A > C and c.2380_2381delCT were identified. Segregation analysis confirmed a paternal origin of the c.117 + 4A > C change and a maternal origin for c.2380_2381delCT (Fig. 5 A). The same compound heterozygous mutations were detected in Patient 4 by Sanger Sequencing. In the unaffected sibling only the mutation c.117 + 4A > C was present. Both *TCIRG1* mutations have not been described before. However, the similar variant c.117 + 4A > T was shown to lead to a use of an upstream cryptic splice donor site [1,21]. According to *in silico* analysis with Human Splicing Finder both variants should have similar effects [8]. The deletion c.2380_2381delCT is predicted to cause a frameshift mutation (p.Ala796fs*34) potentially altering the C-terminus of the protein. The estimated location of the frameshift and splice site mutations are highlighted in the topology model of the a3 subunit of the V-ATPase according to Leng et al. [23] (Fig. 5B).

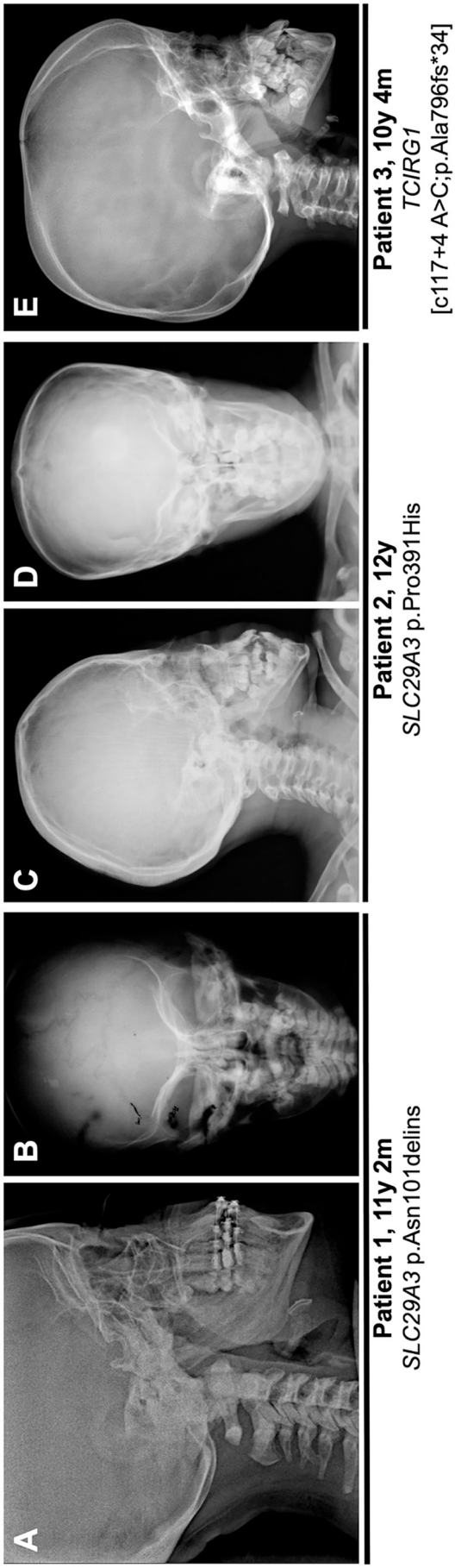

Fig. 3. Cranial radiographs of Patient 1 (A, B) and Patient 2 (C, D), and Patient 3 (E) in occipito-frontal (B), anterior-posterior (D), and lateral (A, C, E) exposure. In Patient 1, osteosclerosis of the skull base is revealed (A), but there is no clear evidence for calvarial thickening (B). Patient 2 shows a flat occiput and mild calvarial thickening (C,D). The skull base is mildly sclerotic. The most pronounced calvarial thickening is seen in Patient 3 (E), but sclerosis of the skull base is also rather mild.

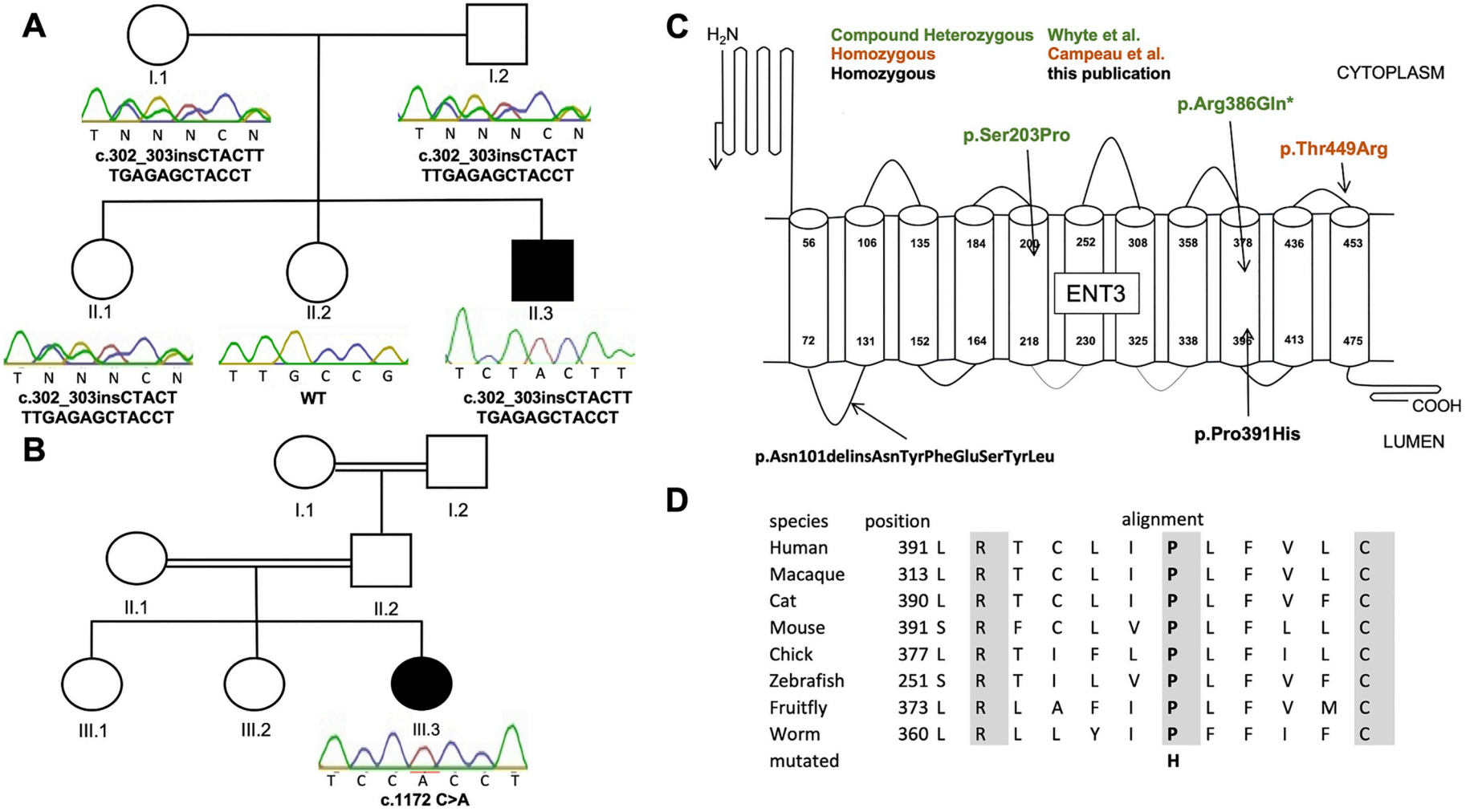

Fig. 4. Pedigrees and sequences of the *SLC29A3* mutations. (A) Pedigree of Patient 1. The index (II.3) with proven *SLC29A3* mutation is shown in black. The parents (I.1, II.2) and the youngest sibling of the index are heterozygous carrier of the mutation. (B) Pedigree of Patient 2. The Index (IV.3) is highlighted in black. Sanger Sequencing of *SLC29A3* confirmed the mutation c.1172 C > A, which is highlighted by an arrow. (C) Topology model of ENT3 encoded by *SLC29A3* consisting of 11 transmembrane helices delineating the effect of the mutations of Patients 1 and 2. Arrows mark the location of the mutations described in this paper and the mutations reported by Whyte et al. and Campeau et al.

4. Discussion

In this study, we describe two homozygous mutations in *SLC29A3* and two compound heterozygous mutations in *TCIRG1* in four individuals with sandwich vertebrae and different degrees of platyspondyly, sclerosis and modeling defects of long bones compatible with the diagnosis mild or intermediate ARO or DOS.

As shown in Table 1 the two patients with osteosclerotic phenotypes and *SLC29A3* mutations previously published by Whyte et al. and Campeau et al. resemble our Patients 1 and 2, although there are some differences [4,36]. The two patients we describe did not have a history of recurrent infections and no skin changes and Patient 2 neither presented with clear metaphyseal widening, nor with pathologic fractures. The absence of any significant skin findings, lymphadenopathy, or hepatosplenomegaly clearly separate Patients 1 and 2 from the histiocytosis-lymphadenopathy plus spectrum [26]. Only in a part of the reported DOS patients, and only in one of the two DOS patients with *SLC29A3* mutations, macular skin changes were found [4,36]. Therefore, our findings cast doubt on the relevance of this clinical feature for the diagnosis of DOS.

Except for Patient 1 with mild concave deformation of vertebrae, the vertebral shape of our patients is more regular and platyspondyly milder than in many described DOS patients [6,13,14,22,34]. The massive metaphyseal flaring present in Patient 3 and 4 is clearly different from the one found in Patients 1 and 2 and reminds of Pyle's disease (OMIM #265900), as already stated in the original description of DOS by Spranger et al. [34]. In contrast to the rather translucent metaphyses in Pyle's disease the flared metaphyses in Patients 3 and 4 are homogenously opaque. However, the intensity and distribution of bone sclerosis in DOS is high heterogeneous. It can strikingly change over time and metaphyses that were first opaque can become translucent after growth has stopped [14]. The DOS patient with the most similar massive metaphyseal flaring is case 1 reported by Elcioglu et al. [9]. The DOS patient depicted by Houston et al. and Lemire et al. displayed not only distal, but also proximal flaring of the femur leading to a widened femoral neck, which is also seen in Patients 1 and 3 [14,22]. The patient with a homozygous *TCIRG1* splice site mutation c.1941 + 5 G > A after exon 15 described by Sobacchi et al. seems very similar to our Patient 3 and 4, although no platyspondyly is explicitly mentioned [32].

Summarizing the findings in 17 patients diagnosed with DOS, Lemire et al. stressed that although the bone changes are not as severe as in infantile malignant osteopetrosis the clinical course also is aggressive and frequently leads to blindness, mental retardation, and even premature death, although bone marrow failure has never been noticed [22]. Two of our patients had evidence for a mild developmental delay, but in none of them vision was affected, which is also true for the two published DOS cases with *SLC29A3* mutations [4,36]. Recently, a patient with sandwich vertebrae, flattening and uneven shape of vertebrae, fractures, and severe long bone modeling defects was described to harbor a homozygous *TNFRSF11A* splice site mutation at position + 3 [13]. Taken together, defining DOS and separating it from the osteopetroses remains a challenge. *SLC29A3* mutations are not specific for DOS, but also cause histiocytosis-lymphadenopathy plus syndrome. Our Patient 2 indicates that sclerosing bone disorders caused by *SLC29A3* mutation do not always fulfill all criteria for DOS. Since also splice site mutations in *TNFRSF11A* and *TCIRG1* can cause flattened sandwich vertebrae and metaphyseal flaring *SLC29A3* mutations are no specific criterion for DOS. Although this suggests that mild mutations in ARO genes in general may cause this phenotype, it is worth noting that for unknown reasons in patients with biallelic *CLCN7* mutations and non-lethal ARO phenotype no platyspondyly has ever been observed [5,7,18]. The clinical features best distinguishing DOS from intermediate ARO is platyspondyly and a more pronounced tubular modeling defect. Since osteopetroses show a strong clinical variability and the therapeutic approach in severe cases is the same, probably no disadvantage would arise if DOS was lumped together with osteopetrosis.

The equilibrative nucleoside transporter 3 (ENT3) encoded by *SLC29A3* resides in lysosomes and mitochondria where it transports nucleosides and nucleotides when pH is acidic [2,29]. The mutation p.Asn101delinsAsnTyrPheGluSerTyrLeu found in Patient 1 is a novelty since no insertions in the coding region of *SLC29A3* have been described to date. It resides in the luminal loop between transmembrane domains 1 and 2, which plays a role in pH activation of ENT3 [29]. Given that the variant p.Met116Arg within this same loop is retained in the ER, it seems likely that this elongated mutant protein shares the same fate [17]. The mutation c.1172C > A (p.Pro391His) found in Patient 2 is nearest to the mutation p.Arg386Gln described in a subject with DOS [4]. Both missense mutations reside in transmembrane helix 9 of ENT3. The exchange of the completely conserved proline residue can be predicted to have severe functional consequences leading to lysosomal accumulation of nucleosides and nucleotides perturbing osteoclast differentiation or function. Our findings underline the great clinical heterogeneity of disorders caused by mutations in *SLC29A3* and the lack of a clear genotype-phenotype correlation. In fact, the mutation p.Arg386Gln (highlighted by * in Fig. 4C) was found in a homozygous state in a patient with histiocytosis-lymphadenopathy plus syndrome [10] and in a heterozygous state in a patient with DOS in combination with a second heterozygous missense mutation [36]. The germline knockout of *Slc29a3* in mice causes a histiocytosis phenotype [15]. Thus, it can be speculated that mutations leading to DOS do not entail a complete loss of ENT3 function. More mutations and functional investigations are needed to get a clearer picture.

TCIRG1 encodes the a3 subunit that anchors the V-ATPase complex to the ruffled membrane of osteoclasts that shares many properties with the lysosomal membrane [33]. It is surprising that the previously published homozygous mutation c.117 + 4A > T causes classical infantile malignant ARO, whereas c.117 + 4A > C in combination with p.Ala796fs*34 entails intermediate ARO [21]. One explanation is increased residual expression of the wildtype transcript from the allele with the splice site alteration. Another explanation could be that p.Ala796fs*34 leads to a stable C-terminally altered protein with retained function. The most similar mutation is p.Glu791fs*27 described by Frattini et al. in a patient with classical ARO [11].

In summary, we add another two cases to the small group of patients with sandwich vertebrae and platyspondyly due to *SLC29A3* mutations. However, our findings also indicate that not all these patients fulfill the criteria for DOS. On the other hand, intermediate ARO due to *TCIRG1* splice site mutations can present with signs of dysosteosclerosis. This underlines the close phenotypic overlap of all osteosclerotic disorders caused by dysfunctional osteoclasts independent of the underlying genetic defect.

Supplementary data to this article can be found online at https://doi.org/10.1016/j.bone.2018.12.002.

Conflicts of interest

None.

Acknowledgments

We are grateful to the patients and family members whose cooperation made this study possible. This study was supported by the Berlin Institute of Health (BIH). This project has received funding from the European Community's Seventh Framework Programme under grant agreement no. 602300 (SYBIL) and the German Federal Ministry of Education and Research (BMBF) within the project “Detection and Individualized Management of Early Onset Osteoporosis (DIMEOS)”.

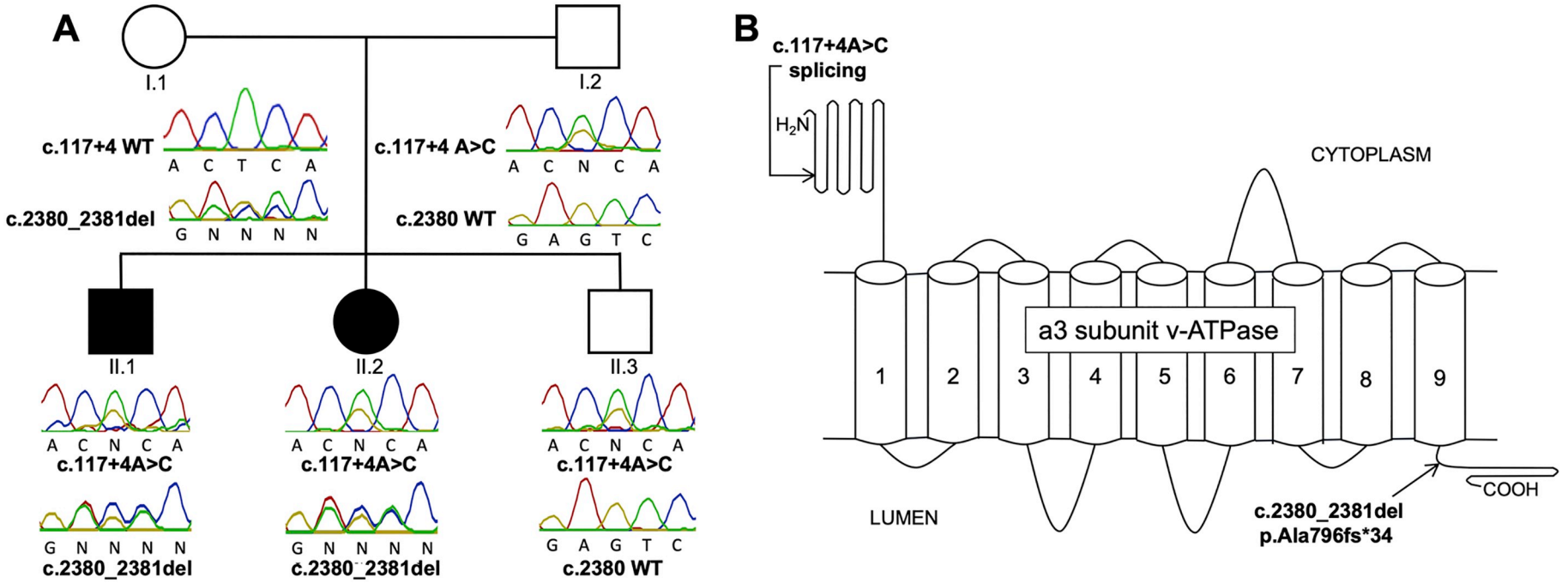

Fig. 5. Pedigree, sequences, topology model and splicing effect illustrating the impact of the *TCIRG1* mutations. (A) Pedigree of the family of patient 3 (II.1) and 4 (II.2). Affected individuals with mutations in *TCIRG1* are shown in black. (B) A model of the V-ATPase a3 subunit according to Leng et al. [9] with the estimated locations of the mutations.

Web resources

The URLs for data presented herein are as follows:
Ensembl Genome Browser, http://www.emsembl.org
Exome Variant Server, NHLBI GO Exome Sequencing Project (ESP), Seattle, WA, http://evs.gs.washington.edu/EVS/
GeneTalk, http://www.gene-talk.de/
Mutation Taster, http://www.mutationtaster.org/
Online Mendelian Inheritance in Man (OMIM), http://www.ncbi.nlm.nih.gov/omim
PolyPhen2, http://genetics.bwh.harvard.edu/pph2/
SIFT, http://sift.jcvi.org/www/SIFT_enst_submit.html
Uniprot, www.uniprot.org
Human Spicing Finder, http://www.umd.be/HSF3/index.html

References

[1] S.L. Anderson, C. Jalas, A. Fedick, K.F. Reid, T.O. Carpenter, D. Chirnomas, N.R. Treff, J. Ekstein, B.Y. Rubin, A founder mutation in the TCIRG1 gene causes osteopetrosis in the Ashkenazi Jewish population, Clin. Genet. 88 (2015) 74–79.

[2] S.A. Baldwin, S.Y. Yao, R.J. Hyde, A.M. Ng, S. Foppolo, K. Barnes, M.W. Ritzel, C.E. Cass, J.D. Young, Functional characterization of novel human and mouse equilibrative nucleoside transporters (hENT3 and mENT3) located in intracellular membranes, J. Biol. Chem. 280 (2005) 15880–15887.

[3] O.D. Benichou, J.D. Laredo, M.C. de Vernejoul, Type II autosomal dominant osteopetrosis (Albers-Schonberg disease): clinical and radiological manifestations in 42 patients, Bone 26 (2000) 87–93.

[4] P.M. Campeau, J.T. Lu, G. Sule, M.M. Jiang, Y. Bae, S. Madan, W. Hogler, N.J. Shaw, S. Mumm, R.A. Gibbs, M.P. Whyte, B.H. Lee, Whole-exome sequencing identifies mutations in the nucleoside transporter gene SLC29A3 in dysosteosclerosis, a form of osteopetrosis, Hum. Mol. Genet. 21 (2012) 4904–4909.

[5] A.B. Campos-Xavier, J.M. Saraiva, L.M. Ribeiro, A. Munnich, V. Cormier-Daire, Chloride channel 7 (CLCN7) gene mutations in intermediate autosomal recessive osteopetrosis, Hum. Genet. 112 (2003) 186–189.

[6] D. Chitayat, K. Silver, E.M. Azouz, Skeletal dysplasia, intracerebral calcifications, optic atrophy, hearing impairment, and mental retardation: nosology of dysosteosclerosis, Am. J. Med. Genet. 43 (1992) 517–523.

[7] E. Cleiren, O. Benichou, E. Van Hul, J. Gram, J. Bollerslev, F.R. Singer, K. Beaverson, A. Aledo, M.P. Whyte, T. Yoneyama, M.C. deVernejoul, W. Van Hul, Albers-Schonberg disease (autosomal dominant osteopetrosis, type II) results from mutations in the ClCN7 chloride channel gene, Hum. Mol. Genet. 10 (2001) 2861–2867.

[8] F.O. Desmet, D. Hamroun, M. Lalande, G. Collod-Beroud, M. Claustres, C. Beroud, Human Splicing Finder: an online bioinformatics tool to predict splicing signals, Nucleic Acids Res. 37 (2009) e67.

[9] N.H. Elcioglu, A. Vellodi, C.M. Hall, Dysosteosclerosis: a report of three new cases and evolution of the radiological findings, J. Med. Genet. 39 (2002) 603–607.

[10] M. Farooq, R.M. Moustafa, A. Fujimoto, H. Fujikawa, O. Abbas, A.G. Kibbi, M. Kurban, Y. Shimomura, Identification of two novel mutations in SLC29A3 encoding an equilibrative nucleoside transporter (hENT3) in two distinct Syrian families with H syndrome: expression studies of SLC29A3 (hENT3) in human skin, Dermatology 224 (2012) 277–284.

[11] A. Frattini, P.J. Orchard, C. Sobacchi, S. Giliani, M. Abinun, J.P. Mattsson, D.J. Keeling, A.K. Andersson, P. Wallbrandt, L. Zecca, L.D. Notarangelo, P. Vezzoni, A. Villa, Defects in TCIRG1 subunit of the vacuolar proton pump are responsible for a subset of human autosomal recessive osteopetrosis, Nat. Genet. 25 (2000) 343–346.

[12] A. Frattini, A. Pangrazio, L. Susani, C. Sobacchi, M. Mirolo, M. Abinun, M. Andolina, A. Flanagan, E.M. Horwitz, E. Mihci, L.D. Notarangelo, U. Ramenghi, A. Teti, J. Van Hove, D. Vujic, T. Young, A. Albertini, P.J. Orchard, P. Vezzoni, A. Villa, Chloride channel ClCN7 mutations are responsible for severe recessive, dominant, and intermediate osteopetrosis, J. Bone Miner. Res. 18 (2003) 1740–1747.

[13] L. Guo, N.H. Elcioglu, O.K. Karalar, M.O. Topkar, Z. Wang, Y. Sakamoto, N. Matsumoto, N. Miyake, G. Nishimura, S. Ikegawa, Dysosteosclerosis is also caused by TNFRSF11A mutation, J. Hum. Genet. 63 (2018) 769–774.

[14] C.S. Houston, J.W. Gerrard, E.J. Ives, Dysosteosclerosis, AJR Am. J. Roentgenol. 130 (1978) 988–991.

[15] C.L. Hsu, W. Lin, D. Seshasayee, Y.H. Chen, X. Ding, Z. Lin, E. Suto, Z. Huang, W.P. Lee, H. Park, M. Xu, M. Sun, L. Rangell, J.L. Lutman, S. Ulufatu, E. Stefanich, C. Chalouni, M. Sagolla, L. Diehl, P. Fielder, B. Dean, M. Balazs, F. Martin, Equilibrative nucleoside transporter 3 deficiency perturbs lysosome function and macrophage homeostasis, Science 335 (2012) 89–92.

[16] T. Kamphans, P.M. Krawitz, GeneTalk: an expert exchange platform for assessing rare sequence variants in personal genomes, Bioinformatics 28 (2012) 2515–2516.

[17] N. Kang, A.H. Jun, Y.D. Bhutia, N. Kannan, J.D. Unadkat, R. Govindarajan, Human equilibrative nucleoside transporter-3 (hENT3) spectrum disorder mutations impair nucleoside transport, protein localization, and stability, J. Biol. Chem. 285 (2010) 28343–28352.

[18] P.N. Kantaputra, S. Thawanaphong, W. Issarangporn, P. Klangsinsirikul, A. Ohazama, P. Sharpe, C. Supanchart, Long-term survival in infantile malignant autosomal recessive osteopetrosis secondary to homozygous p.Arg526Gln mutation in CLCN7, Am. J. Med. Genet. A 158A (2012) 909–916.

[19] U. Kornak, D. Kasper, M.R. Bosl, E. Kaiser, M. Schweizer, A. Schulz, W. Friedrich, G. Delling, T.J. Jentsch, Loss of the ClC-7 chloride channel leads to osteopetrosis in mice and man, Cell 104 (2001) 205–215.

[20] U. Kornak, S. Mundlos, Genetic disorders of the skeleton: a developmental approach, Am. J. Hum. Genet. 73 (2003) 447–474.

[21] U. Kornak, A. Schulz, W. Friedrich, S. Uhlhaas, B. Kremens, T. Voit, C. Hasan, U. Bode, T.J. Jentsch, C. Kubisch, Mutations in the a3 subunit of the vacuolar H(+)-ATPase cause infantile malignant osteopetrosis, Hum. Mol. Genet. 9 (2000) 2059–2063.

[22] E.G. Lemire, S. Wiebe, Clinical and radiologic findings in an adult male with dysosteosclerosis, Am. J. Med. Genet. A 146A (2008) 474–478.

[23] X.H. Leng, T. Nishi, M. Forgac, Transmembrane topography of the 100-kDa a subunit (Vph1p) of the yeast vacuolar proton-translocating ATPase, J. Biol. Chem. 274 (1999) 14655–14661.

[24] C. Letizia, A. Taranta, S. Migliaccio, C. Caliumi, D. Diacinti, E. Delfini, E. D'Erasmo, M. Iacobini, M. Roggini, O.M. Albagha, S.H. Ralston, A. Teti, Type II benign osteopetrosis (Albers-Schonberg disease) caused by a novel mutation in CLCN7 presenting with unusual clinical manifestations, Calcif. Tissue Int. 74 (2004) 42–46.

[25] A. McKenna, M. Hanna, E. Banks, A. Sivachenko, K. Cibulskis, A. Kernytsky, K. Garimella, D. Altshuler, S. Gabriel, M. Daly, M.A. DePristo, The Genome Analysis Toolkit: a MapReduce framework for analyzing next-generation DNA sequencing data, Genome Res. 20 (2010) 1297–1303.

[26] V. Molho-Pessach, I. Lerer, D. Abeliovich, Z. Agha, A. Abu Libdeh, V. Broshtilova, O. Elpeleg, A. Zlotogorski, The H syndrome is caused by mutations in the nucleoside transporter hENT3, Am. J. Hum. Genet. 83 (2008) 529–534.

[27] J. Mrosk, G.S. Bhavani, H. Shah, J. Hecht, U. Kruger, A. Shukla, U. Kornak, K.M. Girisha, Diagnostic strategies and genotype-phenotype correlation in a large Indian cohort of osteogenesis imperfecta, Bone 110 (2018) 368–377.

[28] E. Palagano, H.C. Blair, A. Pangrazio, I. Tourkova, D. Strina, A. Angius, G. Cuccuru, M. Oppo, P. Uva, W. Van Hul, E. Boudin, A. Superti-Furga, F. Faletra, A. Nocerino, M.C. Ferrari, G. Grappiolo, M. Monari, A. Montanelli, P. Vezzoni, A. Villa, C. Sobacchi, Buried in the middle but guilty: intronic mutations in the TCIRG1 gene cause human autosomal recessive osteopetrosis, J. Bone Miner. Res. 30 (2015) 1814–1821.

[29] M.F. Rahman, C. Askwith, R. Govindarajan, Molecular determinants of acidic pH-dependent transport of human equilibrative nucleoside transporter 3, J. Biol. Chem. 292 (2017) 14775–14785.

[30] B.M. Rashid, N.G. Rashid, A. Schulz, G. Lahr, B.F. Nore, A novel missense mutation in the CLCN7 gene linked to benign autosomal dominant osteopetrosis: a case series, J. Med. Case Rep. 7 (7) (2013).

[31] J.M. Schwarz, C. Rodelsperger, M. Schuelke, D. Seelow, MutationTaster evaluates disease-causing potential of sequence alterations, Nat. Methods 7 (2010) 575–576.

[32] C. Sobacchi, A. Pangrazio, A.G. Lopez, D.P. Gomez, M.E. Caldana, L. Susani, P. Vezzoni, A. Villa, As little as needed: the extraordinary case of a mild recessive osteopetrosis owing to a novel splicing hypomorphic mutation in the TCIRG1 gene, J. Bone Miner. Res. 29 (2014) 1646–1650.

[33] C. Sobacchi, A. Schulz, F.P. Coxon, A. Villa, M.H. Helfrich, Osteopetrosis: genetics, treatment and new insights into osteoclast function, Nat. Rev. Endocrinol. 9 (2013) 522–536.

[34] J. Spranger, C. Albrecht, H.J. Rohwedder, H.R. Wiedemann, Dysosteosclerosis–a special form of generalized osteosclerosis, Fortschr Geb Rontgenstr Nuklearmed 109 (1968) 504–512.

[35] K. Wang, M. Li, H. Hakonarson, ANNOVAR: functional annotation of genetic variants from high-throughput sequencing data, Nucleic Acids Res. 38 (2010) e164.

[36] M.P. Whyte, D. Wenkert, W.H. McAlister, D.V. Novack, A.R. Nenninger, X. Zhang, M. Huskey, S. Mumm, Dysosteosclerosis presents as an "osteoclast-poor" form of osteopetrosis: comprehensive investigation of a 3-year-old girl and literature review, J. Bone Miner. Res. 25 (2010) 2527–2539.

[37] X.Y. Zhang, J.W. He, W.Z. Fu, C. Wang, Z.L. Zhang, Novel mutations of TCIRG1 cause a malignant and mild phenotype of autosomal recessive osteopetrosis (ARO) in four Chinese families, Acta Pharmacol. Sin. 38 (2017) 1456–1465.